Shape Changes of the Anterior Lamina Cribrosa in Normal, Ocular Hypertensive, and Glaucomatous Eyes Following Acute Intraocular Pressure Elevation

Tin A. Tun,[1] Sri Gowtham Thakku,[1] Owen Png,[1,2] Mani Baskaran,[1,2] Hla M. Htoon,[1,2] Sourabh Sharma,[1] Monisha E. Nongpiur,[1,2] Ching-Yu Cheng,[1-3] Tin Aung,[1-3] Nicholas G. Strouthidis,[1,4,5] and Michaël J. A. Girard[1,6]

[1]Singapore Eye Research Institute and Singapore National Eye Centre, Singapore
[2]Duke-National University of Singapore Medical School, Singapore
[3]Department of Ophthalmology, Yong Loo Lin School of Medicine, National University of Singapore, Singapore
[4]National Institute of Health Research Biomedical Research Centre, Moorfields Eye Hospital, National Health Service Foundation Trust, and University College London (UCL) Institute of Ophthalmology, London, United Kingdom
[5]Discipline of Clinical Ophthalmology and Eye Health, University of Sydney, Sydney, New South Wales, Australia
[6]Ophthalmic Engineering and Innovation Laboratory, Department of Biomedical Engineering, National University of Singapore, Singapore

Purpose. The purpose of this study was to estimate and compare changes in anterior lamina cribrosa (LC) morphology in normal, ocular hypertensive (OHT), and glaucomatous eyes following acute elevations in intraocular pressure (IOP).

Methods. The optic nerve heads (ONHs) of 97 subjects (17 OHT, 19 primary open-angle glaucoma [POAG], 31 primary angle-closure glaucoma [PACG], and 30 normal subjects) were imaged using optical coherence tomography (OCT). Intraocular pressure was raised twice by applying forces to the anterior sclera, using an ophthalmodynamometer. After each IOP elevation, IOP was held constant and measured; each ONH was rescanned with OCT. In each OCT volume, the anterior LC was enhanced, delineated, and its global shape index (GSI) calculated and compared across groups.

Results. The baseline IOP was 17.5 ± 3.5 mm Hg and was increased to 38 ± 5.9 mm Hg and then to 46.5 ± 5.9 mm Hg. At the first IOP increment, mean GSI was significantly smaller than that at baseline in normal subjects and glaucoma subjects ($P < 0.05$) but not in OHT subjects ($P = 0.12$). For the second IOP increment, the mean GSI was significantly smaller than that at baseline in normal subjects and in OHT eyes ($P < 0.05$). After adjusting for age, sex, and baseline IOP, the LC of POAG eyes was found to be significantly more posteriorly curved than that of normal subjects ($P = 0.04$).

Conclusions. Acute IOP elevations altered anterior LC shape in a complex nonlinear fashion. The LC of POAG eyes was more cupped following acute IOP elevations compared to that of normal subjects.

Keywords: adaptive compensation, glaucoma, global shape index, intraocular pressure elevation, lamina cribrosa, morphometry

Intraocular pressure (IOP) is the only modifiable risk factor for glaucoma; however, its role in the development and progression of glaucomatous optic neuropathy (GON) remains unclear due to the wide range of individual susceptibility of the optic nerve head (ONH) to IOP variations.[1,2] Burgoyne et al.[3] proposed a biomechanical paradigm for glaucoma wherein varied IOP loads induce stresses and strains within the load-bearing connective tissues of the ONH, namely, the lamina cribrosa (LC) and the peripapillary sclera. Within this paradigm, IOP-related stresses and strains are thought to affect axoplasmic transport (at the level of the LC), LC hemodynamics, oxygen and nutrient distributions, and cellular activity within the ONH.[3]

The compliance of the ONH to acute IOP elevation has been studied using experimental[4-14] and computational models,[15-19] and the findings have varied. Studies using either ex vivo or histologic specimens showed that the LC bowed posteriorly in response to acute IOP elevation.[4-6] The in vivo studies[8,10,12] using imaging techniques have also reported that the LC deformed posteriorly from a specific reference plane, namely the plane of Bruch's membrane opening (BMO) following acute IOP elevations. However, Agoumi et al.,[14] in a study of 36 human subjects, found that the LC was not displaced posteriorly following an acute IOP increment. These studies conducted using in vivo imaging techniques estimated the LC deformation from the BMO plane, and many limited their measurements to a few cross-sectional images. This may have led to measurement biases that may explain in part the inconsistencies across studies. Recently, our group introduced a new morphologic measure, the LC global shape index (GSI).[20] This index characterizes the geometrical shape of the anterior LC surface

as a whole from a three-dimensional (3D) ONH reconstruction, and it does not depend on a reference plane (i.e., it is not dependent on reference to the BMO plane). Moreover, because the quantitative score is a single metric, it is easy to understand and compare among different disease classifications.

In this study, we aimed to estimate and compare the structural (shape) changes of the anterior LC (using LC-GSI) in living human eyes (of different diagnoses) following acute IOP elevations.

METHODS

Subject Recruitment

Chinese subjects were recruited from glaucoma clinics at the Singapore National Eye Center, Singapore. Inclusion criteria were subjects ≥50 years of age with phakic eyes, with no known history of intraocular surgery, and no history of penetrating eye trauma. The glaucoma patients were newly diagnosed or receiving pharmacologic treatment, and the subjects with ocular hypertension (OHT) were under observation. We excluded cases with diabetic retinopathy or other optic neuropathies (e.g., optic neuritis), which may account for visual field deficits. All primary angle-closure glaucoma (PACG) eyes had undergone laser peripheral iridotomy prior to recruitment into the study. The study was approved by the SingHealth Centralized Institutional Review Board and adhered to the tenets of the Declaration of Helsinki. Written informed consent was obtained from all subjects.

All participants underwent measurement of visual acuity, refraction using an autokeratometer (RK-5; Canon, Tokyo, Japan), slit-lamp biomicroscopy (model BQ-900; Haag-Streit, Köniz, Switzerland), Goldmann applanation tonometry (model AT900D; Haag-Streit), dark-room 4 mirror gonioscopy (Ocular Instruments, Inc., Bellevue, WA, USA), standard automated perimetry (SAP; SITA-standard 24-2 program; Humphrey Field Analyzer II-750i; Carl Zeiss Meditec, Dublin, CA, USA), 7), IOP measurements with a tonometer (Tonopen AVIA applanation tonometer; Reichert, Inc., Depew, NY, USA) before and after pupillary dilation with tropicamide 1% (Alcon, Puurs, Belgium), and spectral-domain optical coherence tomography (SD-OCT; Spectralis; Heidelberg Engineering, Heidelberg, Germany) imaging before and after acute IOP elevations on the same day.

Glaucoma cases were diagnosed by the presence of GON, defined as vertical cup-to-disc ratio of >0.7 and/or neuroretinal rim narrowing with an associated visual field defect on SAP. The latter defect was defined if the following were found: (1) glaucoma hemifield test result outside normal limits; (2) a cluster of ≥3 nonedge, contiguous points on the pattern deviation plot, not crossing the horizontal meridian, with the probability of <5% being present in age-matched normal subjects (one of which was <1%); and (3) pattern standard deviation <0.05; these were repeatable on two separate occasions; in association with a closed angle (primary angle-closure glaucoma [PACG]) or with an open angle (primary open-angle glaucoma [POAG]). Reliability criteria for SAP were defined as <20% fixation losses, <33% false-negative error, and <33% false-positive error, as recommended by Humphrey Instruments, Inc. (Carl Zeiss). All glaucoma subjects had IOP >21 mm Hg at least once after their GON was clinically diagnosed. OHT was defined by the presence of high IOP (>21 mm Hg) in the absence of GON or visual field loss.

Acute Elevations of Intraocular Pressure and Validation

The safety checks such as patency of laser peripheral iridotomy and postdilation IOP were performed in glaucoma subjects

FIGURE 1. Acute intraocular pressure elevation with the ophthalmodynamometer in place.

before acute IOP elevations. For one eye of each subject, IOP was raised twice by using an ophthalmodynamometer (spring-loaded indenter) that was held perpendicular to the anterior sclera and that gently applies an external force through the temporal side of the lower eye lid (Fig. 1).[14] For each eye, the applied forces were consistently 0.64 N (82.5 g) and 0.9 N (95 g) as calibrated using a uniaxial tensile tester (Instron-5848; Instron, Inc., Noorwood, MA, USA). These forces were chosen as the average forces that corresponded to IOP values of 35 and 45 mm Hg, respectively. (Based on preliminary data obtained from 20 healthy eyes, the mean IOPs for forces of 0.64 N and 0.9 N were 34.35 ± 5.21 mm Hg and 40.48 ± 6.42 mm Hg, respectively).

After each IOP increment, IOP was held constant and measured using the tonometer, while the indenter was maintained in place. Repeatability of the IOP increment was evaluated by performing inter- and intraobserver variability tests on a subset of 20 randomly chosen eyes. For the intraobserver variability, the IOP measurement during acute elevation was repeated on the same eye by the same observer (SS) 15 minutes after the first measurement. For the interobserver variability, two independent observers (TAT and SS) measured the IOP of the same eye in a random sequence with 15-minute intervals.

Optical Coherence Tomography Imaging

The ONH of each subject was imaged 3 times using SD-OCT: before increasing IOP (baseline) and once for each of the 2 IOP elevations (achieved by ophthalmodynamometry). Each OCT volume consisted of 97 serial horizontal B-scans (30-μm
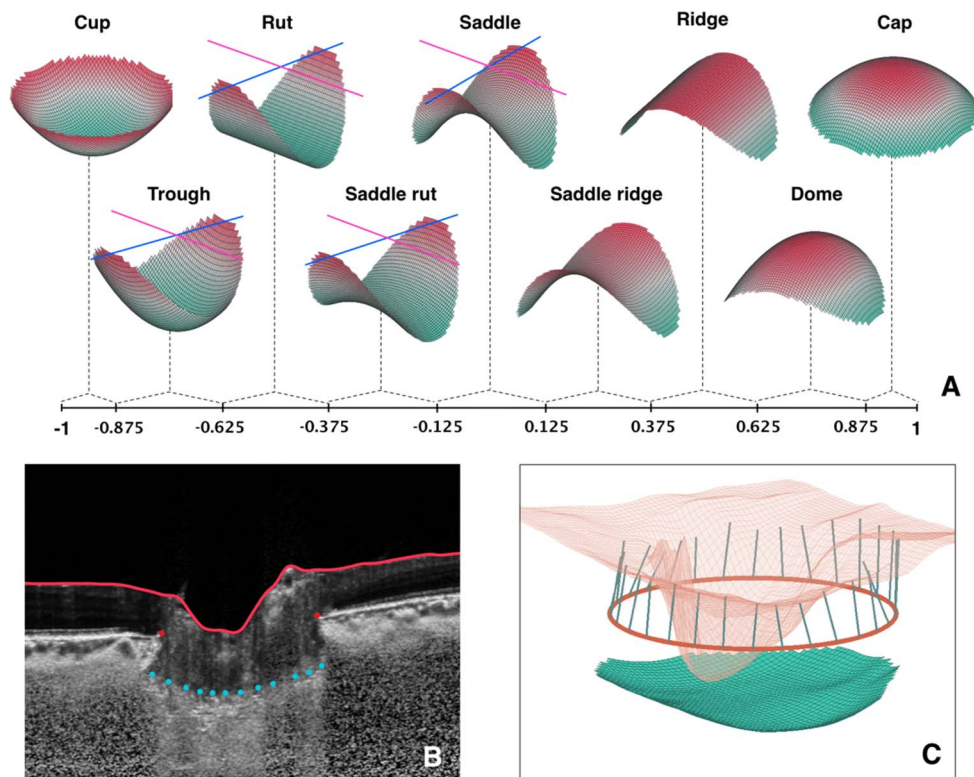
FIGURE 2. Global shape index of lamina cribrosa. (**A**) Global shape index scale with corresponding shape. (**B**) Cross-sectional or 2D view of optic nerve head with delineation of anterior lamina cribrosa and Bruch's membrane opening. (**C**) 3D view of optic nerve head reconstruction.

distance between B-scans; 384 A-scans per B-scan) that covered a rectangular area of $15° × 10°$ centered on the ONH. The eye tracking and enhanced depth imaging modalities of the Spectralis were used during image acquisition. Each B-scan was averaged 20 times during acquisition, and each imaging session with IOP elevation took approximately 2 to 3 minutes.

Image Enhancement, Delineation, and 3D Reconstruction

Raw SD-OCT images were postprocessed and enhanced using adaptive compensation. Such an algorithm has been shown to remove blood vessel shadows, enhance tissue contrast, improve the visibility of the LC, and reduce noise overamplification in the deepest layers of the ONH.[21–23] For each eye, postprocessed OCT volumes were then delineated by a single grader (TAT) using custom-written Matlab (MathWorks, Inc., Natick, MA, USA) algorithms, as previously described.[20] Specifically, the anterior LC and BMO were manually delineated. The position of the anterior LC was defined by a sharp increase in axial signal intensity (corresponding to collagen) extending laterally up to the LC insertion points in the peripapillary sclera.[24] Bruch's membrane opening was defined as the end point of the Bruch's membrane layer on either side of the ONH.[25] The inner limiting membrane was delineated automatically, using Spectralis software.

Using the aforementioned delineations, we used a smoothing spline ("tpaps" function in Matlab software) to generate a best-fitting surface. The smoothing spline contains a smoothing parameter (ranging from 0 to 1) which determines the tolerance or error in fit (0 corresponds to a linear polynomial; 1 to a spline interpolant). This smoothing parameter was chosen to optimize the error in fit with the intraobserver

repeatability, as in our previous publication. This error was measured at approximately 9 μm, which is approximately twice the axial resolution of the OCT scans (4 μm).[20] We reconstructed the ONH structures in 3D, and our customized Matlab algorithms automatically derived the LC-GSI and the LC depth according to established protocols and as described below.[20]

Protocol 1: Lamina Cribrosa-Global Shape Index. LC-GSI was defined as:

$$LC - GSI = \frac{2}{\pi}\tan^{-1}\frac{K_1 + K_2}{K_1 - K_2}(K_1 \geq K_2) \qquad (1)$$

where K_1 and K_2 are the maximum and minimum principal arc curvatures of the LC, respectively. LC-GSI varies between −1, corresponding to a spherical cup (posteriorly curved LC) and +1, a spherical cap (anteriorly curved LC). Lamina cribrosa-GSI was based on global curvature measurements along radial directions. For each radial cross-section, a circular arc was fit to each LC curve as in our previous publication.[20] Figure 2 illustrates various simulated shapes that could be obtained with GSI, and the most common shape of LC in healthy eyes was a saddle rut.[20]

Protocol 2: Lamina Cribrosa Depth. The LC depth was defined as the distance from the BMO reference plane to anterior LC surface, reconstructed from each delineated LC point. The mean depth of all anterior LC points surface was reported as the mean LC depth. Lamina cribrosa-GSI and LC depth were calculated globally. The advantage is that they are less sensitive to local variations due to noise. Our technique allows us to estimate LC shape as a whole without compromising robustness. We derived the root-mean-square error for the intraobserver variability in measurements of LC morphology from our previous publication[20] and root-mean-square error was 8.9 μm for LC depth and 0.05 for LC-GSI.

TABLE 1. Demographic and Clinical Characteristics of the 97 Study Participants

| Characteristic | Mean (± SD) or *n* (%) | | | | *P* value |
	Normal, *n* = 30	OHT, *n* = 30	POAG, *n* = 30	PACG, *n* = 30	
Age, y	61.42 (5.34)	61.78 (5.59)	63.46 (7.96)	68.5 (6.13)	**<0.003***
Females	23 (76.7)	11 (64.7)	3 (15.8)	13 (41.9)	**<0.001†**
IOP at baseline, mm Hg	16.37 (2.71)	20.47 (2.9)	17.74 (3.68)	17 (3.65)	**0.004‡**
IOP at first elevation, mm Hg	37.67 (5.06)	41.53 (5.51)	37.68 (5.51)	36.55 (6.51)	**0.029§**
IOP at second elevation, mm Hg	45.4 (6.43)	48.35 (5.01)	46.47 (5.36)	46.65 (6.22)	0.62
Baseline LC-GSI	−0.21 (0.19)	−0.24 (0.16)	−0.42 (0.21)	−0.33 (0.19)	**<0.024‖**
LC-GSI at first elevation	−0.29 (0.21)	−0.27 (0.18)	−0.43 (0.21)	−0.36 (0.2)	0.1
LC-GSI at second IOP elevation	−0.27 (0.2)	−0.28 (0.2)	−0.44 (0.23)	−0.34 (0.21)	**0.042¶**
Mean deviation of SAP, dB	−1.64 (1.75)	−2.16 (2.69)	−3.12 (4.18)	−5.53 (2.91)	**<0.03***
Mean LC depth from BMO, μm	396.81 (96.24)	388.7 (84.16)	463.77 (159.31)	406.18 (115.61)	0.07
Spherical equivalent, D	−0.38 (3.21)	−1.03 (3.45)	−0.79 (3.46)	−0.18 (2.89)	0.88
Vertical cup-to-disc ratio	0.4 (0.07)	0.54 (0.12)	0.77 (0.12)	0.75 (0.13)	**<0.05#**
Central corneal thickness, μm	551.04 (32.55)	557.21 (45.06)	560.73 (38.26)	538.92 (36.24)	0.25

The analysis of variance with Bonferroni correction was used to compare the differences in the distribution of continuous variables among groups and the chi-square test was used for sex distribution. *P* values in boldface indicate the statistical significance. BMO, Bruch's membrane opening; IOP, intraocular pressure; LC-GSI, lamina cribrosa-global shape index; OHT, ocular hypertension; PACG, primary angle-closure glaucoma; POAG, primary open-angle glaucoma; SAP, standard automated perimetry.

* *P* value is significant between PACG and other diagnoses.
† *P* value is significant among all groups.
‡ *P* value is significant between normal and OHT and between OHT and PACG.
§ *P* value is significant between OHT and PACG.
‖ *P* value is significant between normal and POAG and between OHT and POAG.
¶ *P* value is significant between normal and POAG.
# *P* value is significant among all groups except between POAG and PACG.

Statistical Analysis

Statistical analyses were performed using SPSS version 19.0 software (IBM Corp., Armonk, NY, USA) for Windows (Microsoft, Redmond, WA, USA). Continuous variables were described as the mean ± standard deviation (SD) values. We used analysis of variance (ANOVA) with Bonferroni correction to compare the differences in distribution of continuous variables among groups and the chi-square test for categorical variables. We used Wilcoxon signed ranks test to compare the variables at baseline to those following acute IOP elevations. We used linear mixed model analysis of repeated measures with Bonferroni correction to compare the LC-GSI or LC depth of other groups with normal subjects after adjusting for age, sex, and baseline IOP. Comparison of inter- and intraobserver variability was determined by Bland-Altman analysis using MedCalc v14.12.0 software (Mariakerke, Belgium) for Windows (Microsoft). Statistical significance was set at a *P* value of ≤0.05.

RESULTS

Demographic and Clinical Characteristics

A total of 119 Chinese subjects were recruited, of whom 22 were excluded for the following reasons: 3 had tilted optic discs, 2 had a large peripapillary atrophy, 7 had poor image quality due to cataract or uncorrectable blood vessel shadowing, 1 subject withdrew consent, and 9 subjects had low en-face LC visibility (<50% of BMO area) as estimated from the manual delineations. Therefore, a total of 291 SD-OCT image volumes from 97 subjects (17 subjects with OHT, 19 with POAG, 31 with PACG, and 30 normal subjects) were included, and the mean en-face LC visibility was relatively good (82.9 ± 13.0% of BMO area).

Table 1 shows the demographic and clinical characteristics of the study subjects. Subjects with PACG were significantly older and had higher mean deviation on SAP than those with other diagnoses. The mean vertical cup-to-disc ratios were significantly higher in subjects with POAG (0.77 ± 0.12) and PACG (0.75 ± 0.13) than in normal subjects (0.4 ± 0.07) or OHT subjects (0.54 ± 0.12; all *P* < 0.05).

IOP Baseline Values and Changes With IOP Elevations

Baseline IOP was significantly higher in OHT subjects (20.47 ± 2.9 mm Hg) than in PACG subjects (17.74 ± 3.68 mm Hg) or normal subjects (16.37 ± 2.71 mm Hg) (Table 1). The mean IOP of all study subjects at baseline was 17.5 ± 3.5 mm Hg, which increased to 38 ± 5.9 and then 46.5 ± 5.9 mm Hg, respectively. For each group, the IOP was significantly higher at first or second elevation than at baseline (*P* < 0.001) (Table 2).

LC-GSI Baseline Values and Changes With IOP Elevations

Lamina cribrosa-GSI at baseline was significantly smaller (indicating a more cupped anterior LC) in subjects with POAG (−0.42 ± 0.21) than in normal subjects (−0.21 ± 0.19) or in OHT subjects (−0.24 ± 0.16; *P* < 0.024) (Table 1).

Table 2 shows the median and interquartile ranges of IOP and LC shape and depth at baseline and acute IOP elevations. Compared to baseline, mean LC-GSI significantly decreased at the first IOP increment in normal (−0.21 ± 0.19 vs. −0.29 ± 0.21, respectively; Z = −2.93; *P* = 0.003) and in glaucoma subjects (−0.36 ± 0.2 vs. −0.39 ± 0.21, respectively; Z = −2.13; *P* = 0.033) but not in OHT subjects (−0.24 ± 0.16 vs. −0.27 ± 0.18, respectively; Z = −1.54; *P* = 0.12) (Table 2). For the second IOP increment, mean LC-GSI was significantly smaller than that at baseline in normal (−0.21 ± 0.19 vs. −0.27 ± 0.2, respectively; Z = −2.34; *P* = 0.02) and in OHT (−0.24 ± 0.16 vs. −0.28 ± 0.2, respectively; Z = −2.01; *P* = 0.044) but not in glaucoma subjects (−0.36 ± 0.2 vs. −0.39 ± 0.22, respectively; Z = −0.84; *P* = 0.4) (Table 2). When separating PACG from POAG subjects, no significant LC-GSI changes were seen at IOP increments from that at baseline (all *P* > 0.05).

TABLE 2. Changes in Intraocular Pressure, Lamina Cribrosa Shape, and Depth From Baseline

	Median (IQR) at Baseline	Median (IQR) at IOP elevations	Z Value	P Value*
IOP, mm Hg				
Normal, *n* = 30	16 (2)	37 (6.5)	−4.79	**<0.001**
		44.5 (11)	−4.79	**<0.001**
OHT, *n* = 17	21 (5.5)	42 (9.5)	−3.63	**<0.001**
		48 (7)	−3.63	**<0.001**
Glaucoma, *n* = 50	17 (5)	37 (6.5)	−6.16	**<0.001**
		46 (10)	−6.16	**<0.001**
LC depth, μm				
Normal, *n* = 30	389.31 (107.6)	376.1 (113.43)	−0.13	0.89
		380.2 (113.52)	−0.57	0.57
OHT, *n* = 17	357.66 (108.78)	353.91 (112.83)	−1.44	0.15
		351.98 (118.41)	−0.97	0.33
Glaucoma, *n* = 50	406.63 (200.79)	412.22 (194.56)	−1.95	0.052
		412.5 (197.5)	−0.38	0.7
LC-GSI				
Normal, *n* = 30	−0.22 (0.26)	−0.3 (0.26)	−2.93	**0.003**
		−0.25 (0.32)	−2.34	**0.02**
OHT, *n* = 17	−0.25 (0.22)	−0.27 (0.18)	−1.54	0.12
		−0.28 (0.24)	−2.01	**0.044**
Glaucoma, *n* = 50	−0.38 (0.26)	−0.37 (0.21)	−2.13	**0.033**
		−0.34 (0.34)	−0.84	0.4
POAG, *n* = 19	−0.47 (0.34)	−0.42 (0.36)	−1.03	0.305
		−0.44 (0.36)	−0.2	0.841
PACG, *n* = 31	−0.34 (0.36)	−0.34 (0.27)	−1.8	0.071
		−0.31 (0.3)	−0.59	0.557

Wilcoxon signed rank test was used to detect the difference between two measures. IOP, intraocular pressure; IQR, interquartile range; LC depth, lamina cribrosa depth from the reference plane connecting Bruch's membrane opening; LC-GSI, lamina cribrosa-global shape index; OHT, ocular hypertension; PACG, primary angle-closure glaucoma; POAG, primary open-angle glaucoma.

* *P* values in boldface indicate the statistical significance.

Table 3 shows the directions of LC shape changes compared to baseline. At the first IOP elevation, the LC deformed posteriorly (i.e., more cupped) from its shape at baseline in 10 OHT (58.8%), 11 POAG (57.89%), 20 PACG (64.52%), and 21 normal (70%) subjects. At the second IOP elevation, the LC deformed anteriorly (i.e., less cupped) from its shape at the first elevation in 6 OHT (35.29%), 11 POAG (57.89%), 16 PACG (51.61%), and 17 normal (56.67%) subjects.

After we adjusted for age, sex, and baseline IOP, a mixed model analysis of repeated measures showed that the LC of POAG eyes was significantly more posteriorly curved than that of normal subjects (estimated mean difference, −0.153; 95% confidence interval [CI], −0.498 to −0.318; *P* = 0.041) during acute IOP elevations, but this was not found for other diagnoses compared to normal subjects (Table 4; Fig. 3).

LC Depth Baseline Values and Changes With IOP Elevations

Mean LC depth at baseline was deeper in glaucoma subjects than in OHT or normal subjects, but the difference was not statistically significant (Table 1). No significant changes of LC depth were found at the first or second IOP elevation compared to that at baseline in all groups (Table 2). Lamina cribrosa depth changes during IOP increments were also not significant among groups (Table 4).

Intra- and Interobserver Variability in the First IOP Elevation

Bland-Altman analysis of IOP measurement during first elevation showed that the mean difference was −0.9 (95% CI,

TABLE 3. Summary of the Direction of Lamina Cribrosa Shape Changes Among Groups

	Number of Cases (%)			
Group	Deflected Posteriorly From LC Shape at Baseline	Deflected Anteriorly From LC Shape at Baseline	Deflected Posteriorly From LC Shape at First IOP Elevation	Deflected Anteriorly From LC Shape at First IOP Elevation
Normal	21 (70)	9 (30)	13 (43.33)	17 (56.67)
OHT	10 (58.8)	7 (41.2)	11 (64.71)	6 (35.29)
POAG	11 (57.89)	8 (42.1)	8 (42.11)	11 (57.89)
PACG	20 (64.52)	11 (35.48)	15 (48.39)	16 (51.61)

LC-GSI, lamina cribrosa-global shape index; OHT, ocular hypertension; PACG, primary angle-closure glaucoma; POAG, primary open-angle glaucoma.

TABLE 4. Mixed Model Analysis of Lamina Cribrosa Shape Changes of Different Groups Compared to Normal

Group	Estimated Marginal Mean	95% Confidence Interval	Estimated Marginal Mean Difference Between Normal Subjects and Others	P Value*
LC-GSI				
Normal, *n* = 30	−0.254	−0.329 to −0.18		
OHT, *n* = 17	−0.261	−0.358 to −0.165	−0.007	1
POAG, *n* = 19	−0.408	−0.498 to −0.318	−0.153	**0.041**
PACG, *n* = 31	−0.363	−0.434 to −0.291	−0.108	0.14
LC Depth				
Normal, *n* = 30	389.06	343.82–434.31		
OHT, *n* = 17	389.99	331.7–448.29	0.926	1
POAG, *n* = 19	453.29	398.93–507.64	64.22	0.257
PACG, *n* = 31	422.99	379.66–466.32	33.93	0.91

Linear mixed model analysis of repeated measures with Bonferroni correction was used to compare the LC-GSI or LC depth of other groups with those of normal subjects after adjusting for age, sex and baseline IOP. LC depth, lamina cribrosa depth from the reference plane connecting Bruch's membrane opening; LC-GSI, lamina cribrosa-global shape index; OHT, ocular hypertension; POAG, primary open-angle glaucoma; PACG, primary angle-closure glaucoma.
* *P* value in boldface indicates the statistical significance.

−2.332 to 0.532) for intraobserver variability, and the mean difference was 0.2 (95% CI, −1.998 to 2.398) for interobserver variability. The limit of agreement (LOA) for intraobserver variability was from 5.096 (95% CI, 2.607–7.585) to −6.896 (95% CI, −9.385 to −4.407). The LOA for interobserver variability was from 9.406 (95% CI, 5.585–13.228) to −9.007 (95% CI, −12.828 to −5.185) (Figs. 4A, 4C).

Intra- and Interobserver Variability in the Second IOP Elevation

Bland-Altman analysis of IOP measurement during second elevation showed that the mean difference was −1.35 (95% CI, −3.022 to 0.322) for intraobserver variability, and the mean difference was −0.9 (95% CI, −3.687 to 1.887) for interobserver
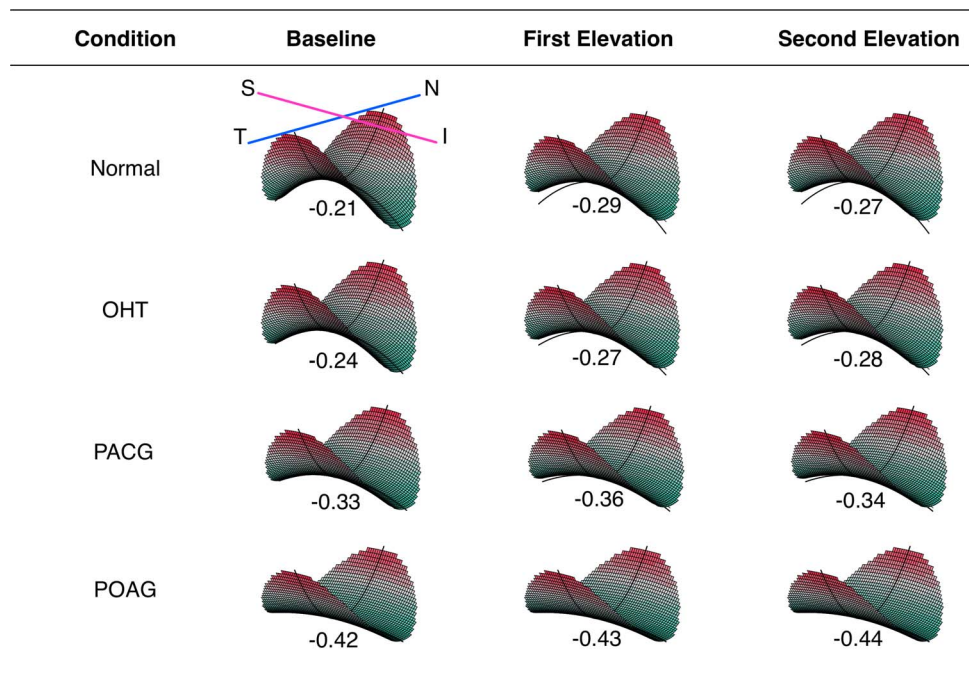

FIGURE 3. Comparison of anterior lamina cribrosa shape changes in normal, ocular hypertensive, and glaucomatous subjects. First elevation is an acute elevation of IOP by applying an external force of 0.64 N or 82.5 g to anterior sclera using an ophthalmodynamometer, and second elevation is by applying a force of 0.9 N or 95 g. Each plot corresponds to the mean anterior lamina shape derived from the mean lamina cribrosa-global shape index (LC-GSI) value (*shown underneath*). *Black lines* represent the outlines of lamina cribrosa's shape at baseline. Moving down each column (Normal to POAG), there is a decrease in LC-GSI corresponding to a deviation from a saddle shape to a cup shape. Similarly, shape changes from the baseline shapes (*black lines*) along the superior-inferior orientation for both IOP elevations are evident in all groups (except POAG). I, inferior; N, nasal; OHT, ocular hypertension; PACG, primary angle-closure glaucoma; POAG, primary open-angle glaucoma; S, superior; T, temporal.
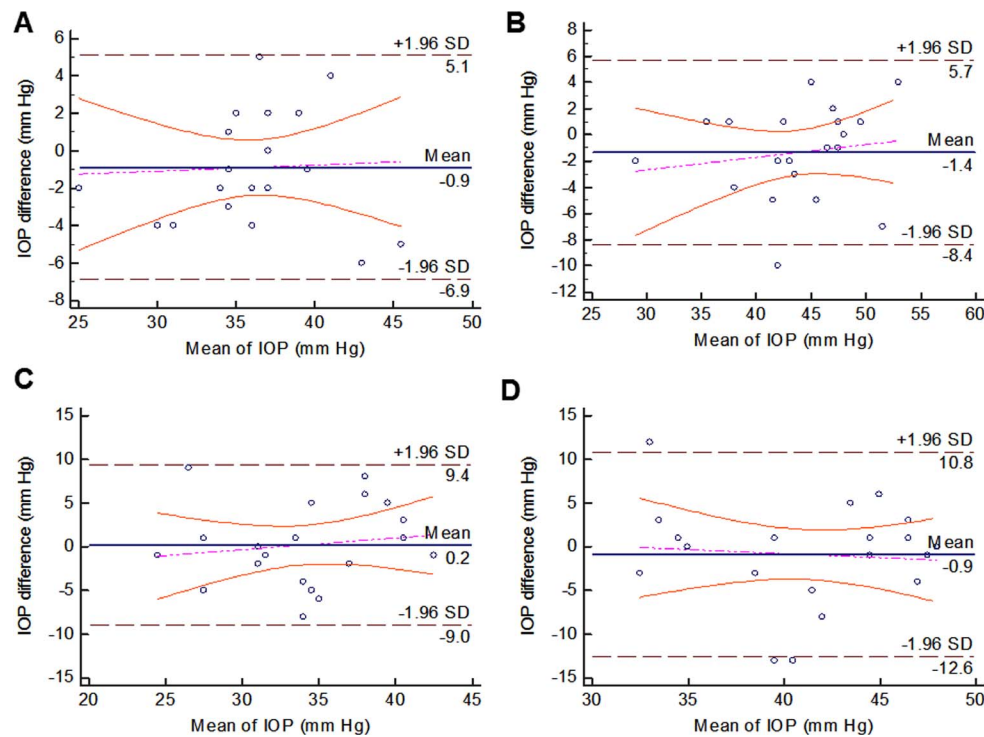
FIGURE 4. Intra- and interobserver repeatability of IOP measurement of acute IOP elevations. IOP, intraobserver repeatability of IOP measurement at first (**A**) and second elevation (**B**). Interobserver repeatability of IOP measurement at first (**C**) and second elevation (**D**).

variability. The LOA for intraobserver variability was from 5.653 (95% CI, 2.746-8.56) to −8.353 (95% CI, −11.26 to −5.446). The LOA for interobserver variability was from 10.772 (95% CI, 5.927-15.617) to −15.572 (95% CI, −17.417 to −7.727) (Figs. 4B, 4D).

DISCUSSION

In this study, we quantified the morphology of the anterior LC, detected by SD-OCT, before and after acute IOP elevations in healthy, ocular hypertensive, and glaucoma subjects. The shape of the anterior LC was characterized using LC depth, a standard "morphologic" parameter, and LC-GSI, a single metric independent of the BMO plane, which can quantify overall LC shape in an intuitive way.[20] We found that the morphology of the anterior LC was significantly changed (as indicated through variations in LC-GSI but not depth) following acute IOP elevations.

More Cupped LCs in Glaucoma at Baseline and Acute IOP Elevations

We noted that the anterior LC in POAG was significantly more cupped (smaller LC-GSI) than that of OHT subjects or normal subjects at baseline. Along with the shape, the LC was also deeper in glaucoma subjects than in subjects with OHT or in normal subjects but the difference was not statistically significant. In an experiment using 25 glaucomatous human eye specimens, Quigley et al.[26] reported that the LC was more cupped in its upper and lower poles in eyes with the most severe glaucoma, resulting in a "W"-shaped morphology; and its thickness also progressively decreased with worsening disease severity. The thickness of LC was not investigated in our cohort because the ability to accurately detect the posterior boundary of the LC in SD-OCT images is controversial. Some studies suggested that the full thickness of LC was

visualized with enhanced depth imaging,[27,28] although others found that challenges remained in accurately detecting the posterior boundary of LC.[29,30]

We found that the LC shape in glaucoma patients was more posteriorly cupped than that of OHT or normal subjects following acute IOP elevations (Fig. 3). Specifically, the LC shape of POAG patients was significantly more posteriorly curved than that of normal subjects. At the first IOP increment, both the glaucoma subjects and normal subjects demonstrated significant alterations in LC shape, which were more cupped than at baseline ("saddle rut"). When separating PACG from POAG subjects, we observed no significant change in LC morphology at IOP increments from that at baseline within each group (all, $P > 0.05$). It might be due to the small sample size in the current study, and future studies with a large sample size will be needed.

In a study conducted in 10 pairs of human specimens (10 experimental eyes and 10 controls), Yan et al.[5] reported that the LC shape was assumed to be "U" shaped and that its bowing increased when the IOP was acutely elevated from 5 to 50 mm Hg. Interestingly, in our study, this finding was not observed in OHT subjects at the first IOP elevation; the LC shape changed significantly only at the second IOP elevation (higher load). This may suggest that the connective tissues of OHT subjects are able to withstand a larger mechanical load than those with glaucoma or from normal subjects. However, such a result will need to be validated using in vivo strain and stiffness mapping techniques as currently established and used in our laboratory.[31,32]

In contrast to the LC shape response to higher load in OHT subjects, the LC in some subjects of the other groups changed their shapes anteriorly (toward a saddle or a cap but not a cup, as illustrated in Fig. 2) at the second IOP elevation from that at first elevation. Studies have also described that acute IOP increments caused LC deformation not only posteriorly but also anteriorly in some cases.[8,10,12,13] It has been hypothesized

that during an acute IOP increase, a stiffer scleral canal deforms less to allow the LC to be deflected posteriorly; whereas a compliant sclera deforms more to pull the LC taut (i.e. deflected anteriorly).[33] The LC may not respond to various IOP loads in isolation but rather the whole ONH including the peripapillary sclera responds as a biomechanical unit. The LC shape change due to acute IOP elevations may be nonlinear and may differ among the different diagnoses.

LC Did Not Change Its Depth Significantly Following Acute IOP Elevations

Interestingly, following acute elevations of IOP, we found that the anterior LC changed its overall shape significantly but not its depth (compared to the BMO reference plane) in all diagnoses. This result was in concordance with previous in vivo studies conducted by Agoumi et al.[14] in 36 human subjects and Strouthidis et al.[13] in 5 monkey eyes. They reported that there was no significant change of LC depth from the BMO reference plane during acute IOP elevation but prelaminar tissue was displaced significantly. This result also highlights the fact that LC depth may not be a good clinical indicator of LC morphology, because multiple LC shapes can exhibit the exact same depth. We believe that more "advanced" shape analysis techniques, like the one presented herein (LC-GSI), should be proposed to establish the implication of LC morphology in the development and progression of glaucoma.

Wu et al.[34] recently reported that chronic IOP increases deepened the anterior LC surface by up to 168.9 µm over a 5-year follow-up period. A longitudinal study, conducted by Strouthidis et al.[35] in 9 nonhuman primates, found that the posterior LC deformation was detected significantly before thinning of retinal nerve fiber layer in mean follow-up of 2.8 months. Therefore, acute changes of the anterior LC surface (LC shape and depth) at the different levels of IOP loads may serve as an early indicator before irreversible nerve damage and vision loss occurs. This interaction may also provide the personalized IOP safety level (or range) of an individual for glaucoma management.

Study Limitations

Some of the limitations in our study include the potential variability of IOP elevations among the observers and the relatively short duration of acute IOP elevations (2–3 minutes); however, the intra- and interobserver variability in our study were good, and we could also detect significant changes of the LC shape within 2 to 3 minutes duration. The current study population was exclusively Chinese, and therefore, the results may not be comparable or extrapolated to other ethnic groups. We calculated LC-GSI globally and estimated the best-fitting arc curvature across entire cross sections. Thus, it may not be sensitive to local LC shape changes due to focal defects such as hemorrhages. Our technique performed better in a simple "U" shape than a complex "W"-shaped LC in a fitting arc.[20] The BMO reference plane may have moved posteriorly (toward the sclera) because of compression of the peripapillary choroid (due to a reduced perfusion) following acute IOP elevations. This may have affected our LC depth measurements and their changes following acute IOP elevations. Finally, limited LC visibility in some SD-OCT images weakened our methodology.

CONCLUSIONS

We demonstrated that acute IOP elevations altered anterior LC shape in living human eyes with a complex nonlinear behavior.

The connective tissues of OHT eyes might be stiffer than those from all other groups because the LC of OHT eyes only changed shape at high IOP. Accordingly, the threshold of IOP to cause alterations in the LC might be higher in eyes with OHT further explaining the resistance toward developing GON. The LC of POAG eyes was more posteriorly curved following acute elevations in IOP compared to that of normal eyes.

References

1. Heijl A, Leske MC, Bengtsson B, Hyman L, Bengtsson B, Hussein M; for the Early Manifest Glaucoma Trial Group. Reduction of intraocular pressure and glaucoma progression: results from the Early Manifest Glaucoma Trial. *Arch Ophthalmol*. 2002;120:1268–1279.

2. Kass MA, Heuer DK, Higginbotham EJ, et al. The Ocular Hypertension Treatment Study: a randomized trial determines that topical ocular hypotensive medication delays or prevents the onset of primary open-angle glaucoma. *Arch Ophthalmol*. 2002;120:701–713.

3. Burgoyne CF, Downs JC, Bellezza AJ, Suh JK, Hart RT. The optic nerve head as a biomechanical structure: a new paradigm for understanding the role of IOP-related stress and strain in the pathophysiology of glaucomatous optic nerve head damage. *Prog Retin Eye Res*. 2005;24:39–73.

4. Levy NS, Crapps EE. Displacement of optic nerve head in response to short-term intraocular pressure elevation in human eyes. *Arch Ophthalmol*. 1984;102:782–786.

5. Yan DB, Coloma FM, Metheetrairut A, Trope GE, Heathcote JG, Ethier CR. Deformation of the lamina cribrosa by elevated intraocular pressure. *Br J Ophthalmol*. 1994;78:643–648.

6. Zeimer RC, Ogura Y. The relation between glaucomatous damage and optic nerve head mechanical compliance. *Arch Ophthalmol*. 1989;107:1232–1234.

7. Bellezza AJ, Rintalan CJ, Thompson HW, Downs JC, Hart RT, Burgoyne CF. Deformation of the lamina cribrosa and anterior scleral canal wall in early experimental glaucoma. *Invest Ophthalmol Vis Sci*. 2003;44:623–637.

8. Yang H, Downs JC, Sigal IA, Roberts MD, Thompson H, Burgoyne CF. Deformation of the normal monkey optic nerve head connective tissue after acute IOP elevation within 3-D histomorphometric reconstructions. *Invest Ophthalmol Vis Sci*. 2009;50:5785–5799.

9. Coleman AL, Quigley HA, Vitale S, Dunkelberger G. Displacement of the optic nerve head by acute changes in intraocular pressure in monkey eyes. *Ophthalmology*. 1991;98:35–40.

10. Roberts MD, Liang Y, Sigal IA, et al. Correlation between local stress and strain and lamina cribrosa connective tissue volume fraction in normal monkey eyes. *Invest Ophthalmol Vis Sci*. 2010;51:295–307.

11. Fortune B, Choe TE, Reynaud J, et al. Deformation of the rodent optic nerve head and peripapillary structures during acute intraocular pressure elevation. *Invest Ophthalmol Vis Sci*. 2011;52:6651–6661.

12. Sigal IA, Yang H, Roberts MD, et al. IOP-induced lamina cribrosa deformation and scleral canal expansion: independent or related? *Invest Ophthalmol Vis Sci*. 2011;52:9023–9032.

13. Strouthidis NG, Fortune B, Yang H, Sigal IA, Burgoyne CF. Effect of acute intraocular pressure elevation on the monkey optic nerve head as detected by spectral domain optical coherence tomography. *Invest Ophthalmol Vis Sci*. 2011;52:9431–9437.

14. Agoumi Y, Sharpe GP, Hutchison DM, Nicolela MT, Artes PH, Chauhan BC. Laminar and prelaminar tissue displacement during intraocular pressure elevation in glaucoma patients and healthy controls. *Ophthalmology*. 2011;118:52–59.

15. Girard MJ, Downs JC, Burgoyne CF, Suh JK. Peripapillary and posterior scleral mechanics—part I: development of an anisotropic hyperelastic constitutive model. *J Biomech Eng*. 2009;131:051011.

16. Zhang L, Albon J, Jones H, et al. Collagen microstructural factors influencing optic nerve head biomechanics. *Invest Ophthalmol Vis Sci*. 2015;56:2031–2042.

17. Grytz R, Sigal IA, Ruberti JW, Meschke G, Downs JC. Lamina cribrosa thickening in early glaucoma predicted by a microstructure motivated growth and remodeling approach. *Mech Mater*. 2012;44:99–109.

18. Sigal IA, Flanagan JG, Tertinegg I, Ethier CR. Modeling individual-specific human optic nerve head biomechanics. Part I: IOP-induced deformations and influence of geometry. *Biomech Model Mechanobiol*. 2009;8:85–98.

19. Sigal IA, Flanagan JG, Tertinegg I, Ethier CR. Modeling individual-specific human optic nerve head biomechanics. Part II: influence of material properties. *Biomech Model Mechanobiol*. 2009;8:99–109.

20. Thakku SG, Tham YC, Baskaran M, et al. A global shape index to characterize anterior lamina cribrosa morphology and its determinants in healthy Indian eyes. *Invest Ophthalmol Vis Sci*. 2015;56:3604–3614.

21. Mari JM, Strouthidis NG, Park SC, Girard MJ. Enhancement of lamina cribrosa visibility in optical coherence tomography images using adaptive compensation. *Invest Ophthalmol Vis Sci*. 2013;54:2238–2247.

22. Girard MJ, Strouthidis NG, Ethier CR, Mari JM. Shadow removal and contrast enhancement in optical coherence tomography images of the human optic nerve head. *Invest Ophthalmol Vis Sci*. 2011;52:7738–7748.

23. Girard MJ, Tun TA, Husain R, et al. Lamina cribrosa visibility using optical coherence tomography: comparison of devices and effects of image enhancement techniques. *Invest Ophthalmol Vis Sci*. 2015;56:865–874.

24. Strouthidis NG, Grimm J, Williams GA, Cull GA, Wilson DJ, Burgoyne CF. A comparison of optic nerve head morphology viewed by spectral domain optical coherence tomography and by serial histology. *Invest Ophthalmol Vis Sci*. 2010;51:1464–1474.

25. Tun TA, Sun CH, Baskaran M, et al. Determinants of optical coherence tomography-derived minimum neuroretinal rim width in a normal Chinese population. *Invest Ophthalmol Vis Sci*. 2015;56:3337–3344.

26. Quigley HA, Hohman RM, Addicks EM, Massof RW, Green WR. Morphologic changes in the lamina cribrosa correlated with neural loss in open-angle glaucoma. *Am J Ophthalmol*. 1983; 95:673–691.

27. Kim S, Sung KR, Lee JR, Lee KS. Evaluation of lamina cribrosa in pseudoexfoliation syndrome using spectral-domain optical coherence tomography enhanced depth imaging. *Ophthalmology*. 2013;120:1798–1803.

28. Lee EJ, Kim TW, Weinreb RN, Park KH, Kim SH, Kim DM. Visualization of the lamina cribrosa using enhanced depth imaging spectral-domain optical coherence tomography. *Am J Ophthalmol*. 2011;152:87–95.

29. Girard MJ, Tun TA, Husain R, et al. Lamina cribrosa visibility using optical coherence tomography: comparison of devices and effects of image enhancement techniques. *Invest Ophthalmol Vis Sci*. 2015;56:865–874.

30. Sigal IA, Wang B, Strouthidis NG, Akagi T, Girard MJ. Recent advances in OCT imaging of the lamina cribrosa. *Br J Ophthalmol*. 2014;98(suppl 2):ii34–9.

31. Girard MJ, Beotra MR, Chin KS, et al. In vivo 3-dimensional strain mapping of the optic nerve head following intraocular pressure lowering by trabeculectomy. *Ophthalmology*. 2016; 123:1190–1200.

32. Girard MJ, Strouthidis NG, Desjardins A, Mari JM, Ethier CR. In vivo optic nerve head biomechanics: performance testing of a three-dimensional tracking algorithm. *J R Soc Interface*. 2013; 10:20130459.

33. Crawford Downs J, Roberts MD, Sigal IA. Glaucomatous cupping of the lamina cribrosa: a review of the evidence for active progressive remodeling as a mechanism. *Exp Eye Res*. 2011;93:133–140.

34. Wu Z, Xu G, Weinreb RN, Yu M, Leung CK. Optic nerve head deformation in glaucoma: a prospective analysis of optic nerve head surface and lamina cribrosa surface displacement. *Ophthalmology*. 2015;122:1317–1329.

35. Strouthidis NG, Fortune B, Yang H, Sigal IA, Burgoyne CF. Longitudinal change detected by spectral domain optical coherence tomography in the optic nerve head and peripapillary retina in experimental glaucoma. *Invest Ophthalmol Vis Sci*. 2011;52:1206–1219.

Investigative Ophthalmology & Visual Science